FAILURE CHARACTERISTICS OF REINFORCED CONCRETE BEAMS REPAIRED WITH CFRP COMPOSITES

Yongtao Dong, University of Illinois at Chicago, Chicago, IL
Ming Zhao, Tongji University, Shanghai, China
Farhad Ansari, University of Illinois at Chicago, Chicago, IL

Abstract

The flexural performance of reinforced concrete beams with externally bonded carbon fiber reinforced polymer (CFRP) fabrics were studied in terms of fabric length and thickness. The internal steel reinforcement ratio and preloading on the behavior of the strengthened beams are discussed. It was found that attaching of CFRP system to the tension surface of either pre-cracked or un-cracked beams improve the load-carrying capacity and stiffness of the flexural beams while unexpected failure modes, such as the peeling of concrete cover and the debonding between the CFRP fabric and concrete still occur. The causes and mechanisms involved in these types of failure modes are investigated. The ultimate strains of the steel reinforcement at failure were on the average about 2.5 times that of yield strain for steel. Therefore, despite the eventual peeling of the concrete cover and debonding of the fabric, the retrofitted beams have capability for considerable deflections.

Keywords: Reinforced concrete; Carbon fiber reinforced polymer; Strengthening; Failure mode

Introduction

The growing interest in fiber-reinforced polymer (FRP) system in strengthening and retrofit is becoming apparent in recent years because of the special properties of these composite materials. In general, FRP materials are lightweight, none corrosive, and exhibit high tensile strength. Additionally, these materials are readily available in several forms ranging from factory made laminates to dry fiber sheets that can be wrapped to conform to the geometry of a structure. These attributes provide opportunities for FRP composites to be used as alternatives to the traditional materials such as externally bonded steel plates, steel or concrete jackets in strengthening or retrofitting of existing concrete structures.

In flexural strengthening, the FRP reinforcement can be externally bonded to the tension face of the members with fibers oriented along the length of the member to provide an increase in flexural capacity. Despite the many advantages of FRP strengthened reinforced concrete (RC) flexural members, their ultimate failure may occur in a brittle manner due to sudden debonding of the FRP system from the concrete. Such a failure mode not only diminishes the strengthening potential of externally bonded FRP system but it is also unacceptable from the point of view of structural safety. The premature FRP debonding failure has been experimentally identified by a number of investigators, including Swamy and Mukhopadhaya [1], Sharif et al. [2], Arduini and Nanni [3-4], Norris et al. [5], GangaRao and Vijay [6], Ross et al. [7], Rahimi and Hutchinson [8], Nguyen et al. [9]. Debonding failure can be classified into two distinct categories: (a) the failure that occurs in the zone of high bending moment and low shear force; and (b) the failure that originates at or near FRP system cutoff end in a region of high shear force and low bending moment. While FRP system debonding in the first category is often very local, the latter type, which occurs almost exclusively near the FRP system cutoff end, is due to high stress concentrations in the interface layer. The shear crack at the cutoff end causes an eccentricity between the tension force in the external FRP and the forces in the beam, which leads to peeling of the concrete

cover. This peeling failure occurs because the FRP plate (sheet) is not continuous over the support and adequate anchorage lacks at the FRP system ends. Research results [1, 2, 4, 10 and 11] have shown that properly designed anchorage systems at the FRP ends can eliminate peeling failure.

Recently, Bonacci et al. [12] compiled and analyzed a total of 127 FRP strengthened RC beams from 23 separate studies. Results of the study included an analysis of trends in failure mode, strength gain, and deformability. One-third of the specimens showed strength increases of 50% or more in combination with considerable deflection capacity. Failure by debonding of FRP was prevalent among the specimens studied. Sixty-three percent of failures were attributed to debonding of FRP. In the majority of cases, it was not possible to distinguish among the various modes of debonding, i.e., at cutoff point, in vicinity of load point, or due to fault at a shear crack.

Ultimate flexural strength of the strengthened beam should generally be controlled by rupture of the FRP or compression crushing of the concrete with yielding of the internal steel reinforcement. The interrelationships between strength, failure mode, and deflection capacity of beams with FRP flexural reinforcement must be understood. Therefore, the problem remains as how to guard against unwanted failure modes and ensure ample deflection capacity. The premature plate (sheet) debonding failures are of brittle nature and need to be investigated further. The work presented here pertains to a series of laboratory tests aimed at development of basic understanding as to the effects of strengthening parameters on the performance of RC beams with externally bonded FRP systems. The parameters investigated included: failure mode, strengthening efficiency, strength gain, and deformability of strengthened beams.

Experimental Program

Description of Specimens

Typical RC beam dimensions and steel reinforcement details are shown in Fig. 1. Type I Portland cement was used in all the mixtures. The mix proportion of constituents by weight was 1 : 0.43 : 2.20 : 2.97, which corresponded to cement, water, sand and gravel. The average 28-day concrete compressive strength for all the beams was 38.2MPa. The longitudinal steel reinforcement consisted of 16mm and 10mm diameter Grade 60 standard rebars having a yielding strength of 0.41 GPa. The transverse reinforcement consisted of 6mm diameter Grade 40 smooth bars. All beams were 152.4 3 304.8 mm in cross section and 3.048 m long, having a nominal tension steel depth of 253 mm. The specimens were designed as per ACI 318-99 design guideline [13].
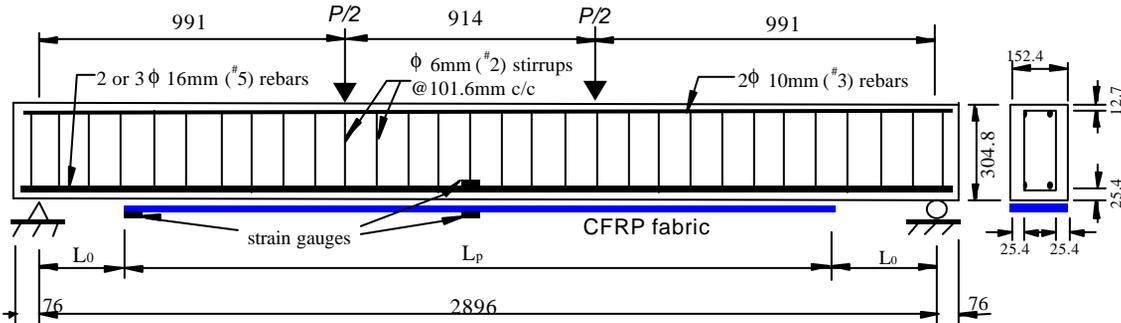

Fig. 1. Details of RC Beam with Externally Bonded CFRP Fabric (Units: mm)

CFRP Strengthening Schemes

The carbon fiber reinforced polymer (CFRP) composite employed in this study was manufactured by Sika Corporation (SikaWrap Hex 103C). This fabric, with a width of 90 mm and a thickness of 1 mm, is a high strength, unidirectional carbon fiber. The fabric is field impregnated with SikaDur 330 epoxy to form a carbon fiber reinforced polymer (CFRP) system. As per manufacturer's data, the tensile strength and modulus of elasticity of the fabric were 3,450MPa and 234,500MPa, respectively, with an elongation of 1.5 percent. The CFRP system (SikaWrap 103C fabric and resin) had a strength of 960MPa, a modulus of elasticity of 73,100MPa, and an elongation of 1.33 percent.

To obtain a rough surface the tension face of the RC beam was sand-blasted and the dust particles were removed by airbrush. The finished concrete surface was characterized as a uniformly abraded surface with exposed small- to medium-sized pieces of aggregate.

The epoxy components were mixed at site according to the instructions provided by the producer. The epoxy paste was then troweled into position on the surface of the concrete specimen. The fabric, which was previously cut to the required dimensions (the width was the same as the cross-sectional width of the RC beam and their lengths varied), was put on the prepared surface with their fibers oriented in the longitudinal direction of the beam. By using a roller brush, the CFRP fabrics were gently pressed along the fiber direction to achieve uniform fiber-wetting and to remove the air bubbles. The beams were cured in laboratory environment. The specimen variables included the number of CFRP plies, the length of the CFRP fabrics and the main internal steel reinforcement. The specimen details are given in Table 1. Beam B0 was the control beam, without additional CFRP strengthening, while all the other beams were strengthened with the fabric. The nominal thickness of CFRP system (epoxy and composite) for one layer was 2 mm.

Table 1. Steel Reinforcement and CFRP of the Beams

Beam No. (1)	Number of ϕ16mm steel rebar (2)	CFRP Thickness (mm) (3)	CFRP Length (mm) (4)	Distance from CFRP end to support (mm) (5)
B0	2	NA	NA	NA
B1	2	2	2134	381
B2	2	2	2286	305
B3	2	2	2744	76
B4	2	2	2744	76
B5	2	4	2134	381
B6	3	4	2134	381

Testing Setup and Procedure

All the beams were tested under four-point bending in the structural testing frame. The specimens were spanned at 2.9 m and loaded symmetrically about their centerline at two points of 0.914 m apart (Fig.1). Deflections at mid-span were measured by two LVDTs (linear variable differential transformer) on the two sides of the beam. Dial gauges were installed at the support points to measure their vertical displacements. The readings from LVDTs and dial gages were used to calculate the actual deflection at the mid-span. The deformations of the main longitudinal steel reinforcement and CFRP sheet were measured by electrical resistance strain gauges (Fig.1).

Prior to the actual tests, the specimens were initially loaded to a small fraction (about 5%) of the design ultimate load then unloaded so as to stabilize the beam and to prevent any possible twisting. The transducers and gauges were then zeroed and the actual test started under displacement control. At every

deformation increment, data from the transducers and gauges were acquired by a data acquisition system. To simulate service conditions of beam under service load, all of the strengthened beams except B4 were preloaded to cracking prior to the application of CFRP fabric. The preloading was applied approximately up to the cracking load (Table. 2) which allowed the formation of several cracks in the region of constant moment. The fabric was then adhered to the specimen under the sustained load. Following the curing period, load was applied monotonically until failure.

Flexural Analysis of CFRP Strengthened Beam

Flexural analyses were made to estimate the nominal flexural capacity of both conventional RC and FRP strengthened RC beams. The flexural capacity of strengthened beams depends on the control failure modes [14], which include: (a) concrete crushing before yielding of the reinforcing steel (concrete crushing failure); (b) yielding of the steel in tension followed by FRP system rupture (FRP rupture); and (c) yielding of the steel in tension followed by concrete crushing (tension failure). For a given RC beam, if the required increase of moment capacity for the FRP strengthened beam is relatively small, then the required FRP cross-sectional area will also be small. This may yield a design for which FRP rupture occurs before the concrete attains the ultimate compressive strain, thus resulting in a less ductile failure. Therefore, in such cases a minimum amount of FRP, $A_{f,min}$, should be provided to preclude the FRP rupture failure. On the other hand, if more FRP is used, the concrete crushing may occur prior or just following the yielding of reinforcing steel. At this time, a maximum amount of FRP, $A_{f,max}$, should be provided to avoid premature crushing of concrete. $A_{f,max}$ and $A_{f,min}$ can be determined by simulating the strain conditions defined by the balanced conditions between the different failure modes [15]. Beams tested in this study were designed to fail in tension since the cross-sectional areas of FRP fabrics were between the maximum and minimum requirements (Appendix I). In the analysis, the stress-strain response of FRP and steel were considered linear elastic and elastic perfectly plastic, respectively. The Park and Paulay numerical approximation [16] of the Hognestadt stress block was employed to calculate the stress in concrete. Full composite action between FRP and RC beam was assumed. The flexural capacity of the beams under tension failure conditions were evaluated and listed in Table 2 (see Appendix I for details).

Table 2. Loads and Deflections of the Beams at Failure

Beam No. (1)	Load When FRP Applied (kN) (2)	Ultimate Load (kN) (3)	Mid-span Deflection (mm) (4)	Strength Ratio SR (5)	Deflection Ratio DR (6)	Predicted Load (kN) (7)	Failure Mode (8)
B0	-	96.59	70.17	1.00	1.00	85.53	flexural
B1	28.18	148.20	31.86	1.53	0.45	188.80	peeling
B2	23.29	157.95	24.31	1.64	0.17	188.80	peeling
B3	0.00	183.79	34.17	1.90	0.52	188.80	debonding
B4	25.83	188.05	34.70	1.95	0.49	188.80	peeling
B5	24.07	178.40	20.40	1.85	0.35	228.35	peeling
B6	26.23	181.72	20.97	1.88	0.29	240.94	peeling

Discussion of Experimental and Analytical Results

Strength and Deformability

Experimental results as well as the predicted flexural capacity of the beams are given in Table 2. Fig. 2 shows the load-deflection behaviors of the beams. The ultimate load represents the sum of the two equal concentrated loads at failure. All the beams showed at first, a linear-elastic behavior followed by appearance of several cracks in the mid-span region of the beam. Thereafter, a non-linear phase was recorded with the development of numerous flexural cracks and considerable deflections. As the load increased, the stiffness of the beam changed dramatically with the yielding of the internal steel reinforcements. Beam B0, the control beam, reached failure by crushing of the concrete long after the yielding of the steel. All the other beams showed either a peeling failure of the concrete cover or a debonding failure at the interface of FRP and concrete during yielding of the steel reinforcements. As shown in Table 2 and Fig. 2, in terms of strength and stiffness, all the beams with externally bonded FRP system performed significantly better than the control (un-strengthened) beam. The strength of RC beams strengthened with external FRP system is influenced by the original stiffness of the beams, the amount of external FRP sheet and the adhesion between the concrete and the FRP.
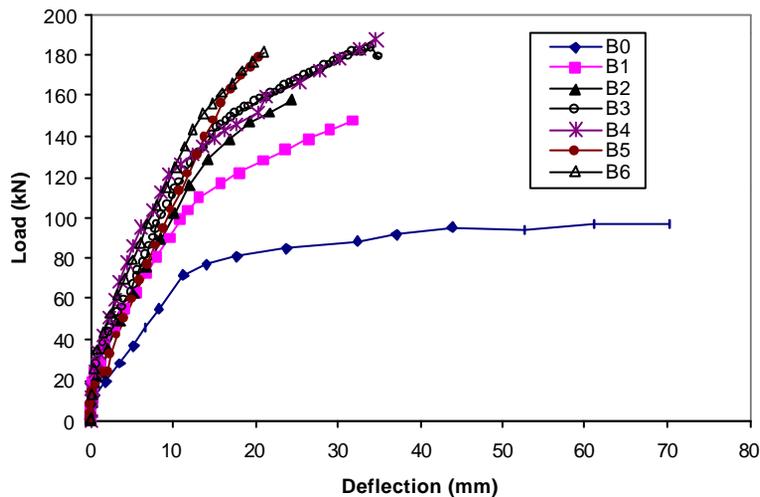

Fig. 2. Load-Deflection Behavior of Tested RC Beams

Two indices can be used to compare the performance of the strengthened beam with its conventionally reinforced counterpart: the strengthening ratio (SR) and the deflection ratio (DR). SR is the ratio of the strength of beam with FRP to the strength of control beam. In a similar manner, DR pertains to the ratio of the deflections at ultimate load for the FRP and control beams, respectively. Strengthening ratios varied from 1.53 to 1.95 and deflection ratios from 0.17 to 0.52 (Table 2). This indicates that increased load capacities of the strengthened beams were accompanied by substantial losses in deflection capability. All the strengthened beams failed in an abrupt manner through peeling of the concrete cover. Theoretical predictions of strength were based on strain compatibility methods (Appendix I) and assumption of full composite action between the FRP and the concrete. However, theoretical solutions overestimated strength of the beams, which generally failed prematurely. Peeling and debonding occurred at loads lower than those predicted by the conventional design equations (Table 2). In both cases, the stiffening/strengthening resources of the FRP system were not fully utilized and therefore all the failures occurred prematurely. This indicated that full composite action had not been developed prior to failure.

Effect of the Fabric Length

Beam B1, B2 and B3 were strengthened with various fabric lengths. Their load and mid-span deflection relationships are shown in Fig. 3. The failure loads for beam with the longer fabric that extends very close to the supports (beam B3) was much higher than for beams with shorter fabrics (beams B1 and B2). The failure modes were also different. B3 failed by debonding, while B1 and B2 failed through peeling.

Effect of Preloading

Beam B4 was virgin prior to strengthening by FRP. Observation of load versus deflection of beam B3 and B4 indicated no significant variation in the ultimate load-carrying capacities of the pre-cracked and un-cracked beams (Fig. 4). Similar observations were found in the bending tests of RC beams wrapped with carbon fabric [6] and RC beams strengthened with CFRP sheets [3]. The pre-loading pertained only to low service load of the cracking load of the control beam. Other researchers reported increase in ultimate loads after strengthening of severely damaged RC beam [2].
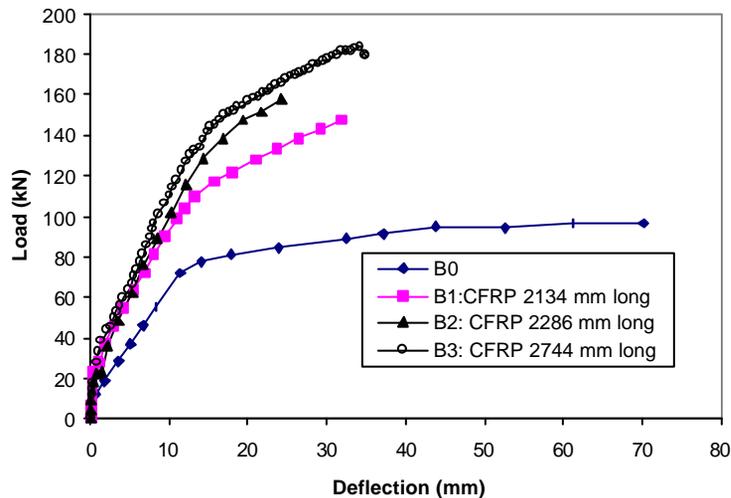

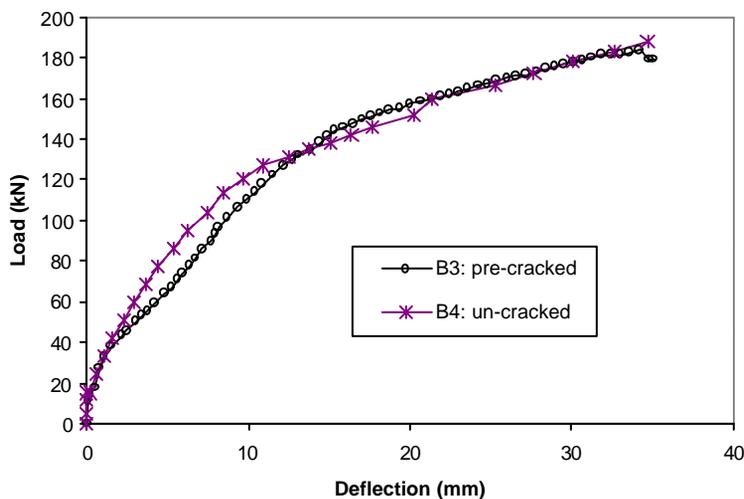**Fig. 3.** Load-Deflection Behavior of Beams with Various Fabric Lengths

Fig. 4. Comparison of Pre-cracked and Un-cracked CFRP-Strengthened Beams

6

Effect of CFRP Thickness

For beams B1 and B5, all the parameters were kept the same except for the thickness of fabrics. Beam B5 with fabric thickness of 4 mm (two layers) demonstrated higher strength and stiffness after cracking, and lower ductility than that of beam B1 with 2 mm (one layer) of fabric (Fig. 5).

Effect of Reinforcement Ratio

Beams B5 and B6 were reinforced with two and three rebars respectively. As shown in Fig. 6, the difference in steel reinforcement ratio resulted in reduced stiffness for B5, and not much of decrease in the ultimate load carrying capacity. This is due to the fact that the stiffness is dependent on both the internal steel reinforcement and external CFRP reinforcement while the ultimate load is determined by the control failure mode of concrete cover peeling which is independent of the internal steel reinforcement.
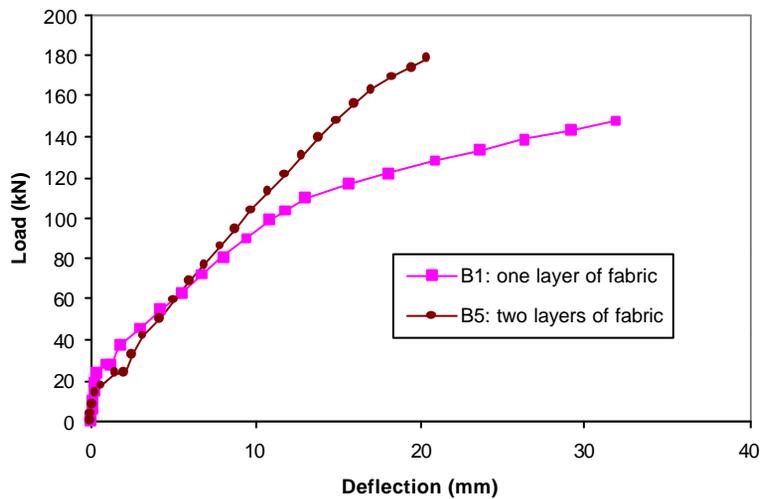

Fig. 5. Load-Deflection Behavior of Beams with Different Fabric Thickness
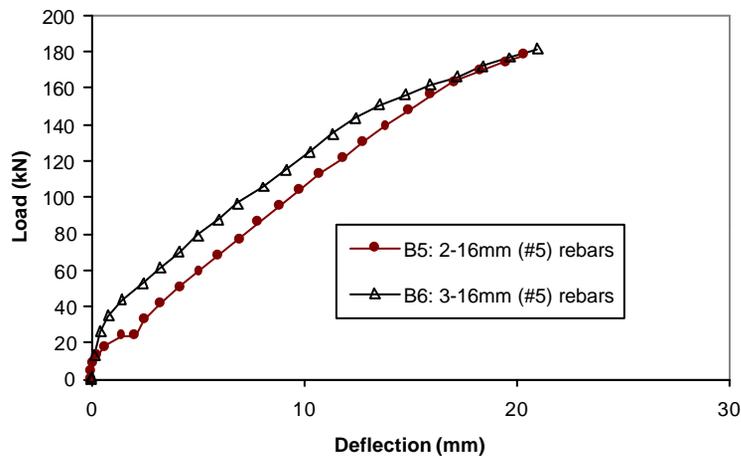

Fig. 6. Load-Deflection Behavior of Beams with Different Steel Reinforcement

Failure Modes

As seen from the above experimental results, the control beam failed by concrete crushing during the yielding of the internal steel reinforcement. The strengthened beams failed either by peeling of the concrete cover from the CFRP fabric cutoff points (Fig. 7) or debonding of the CFRP fabric at the locations of flexural cracks (Fig. 8), although all of these beams were designed to fail in flexure. Both failure types occurred in a brittle explosive manner. Flexural cracks were observed to be uniformly distributed within the fabric-bond zone on the tension face. The cracks were narrower in the strengthened beams as compared to those observed in control beam due to the presence of the CFRP fabric at the concrete surface.
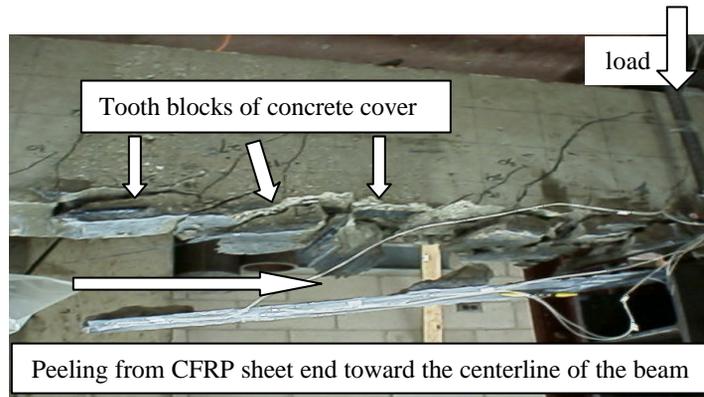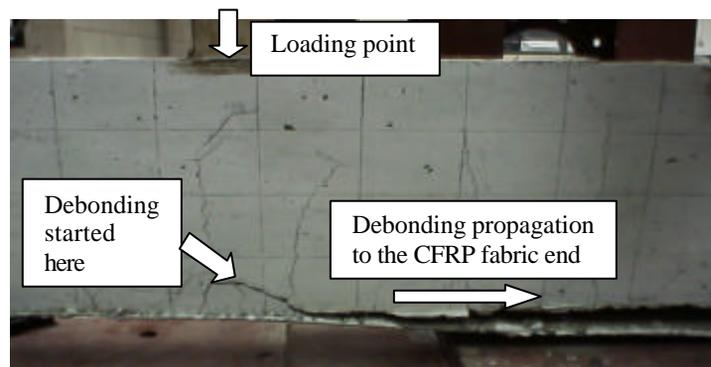

Fig. 7. Peeling Failure of Concrete Cover (Beam B2)

Fig. 8. Debonding Failure between FRP Fabric and Concrete (Beam B3)

Peeling Failure

The application of the CFRP fabrics to the soffit of the concrete beam introduces shear transfer to the concrete/epoxy interface. At the termination of the CFRP fabric, a change in stiffness and discontinuity of beam curvature creates a stress concentration in the concrete, often initiating cracks that can lead to debonding.

Based on the experimental observations, the mechanism of peeling failure can be described in the following sequences:

1) uniformly spaced cracks developed in the constant bending moment zone and some small cracks in the shear span (Fig. 9a);

2) as a result of shear stress and normal stress concentrations at the CFRP fabric end, the concrete rupture strength was exceeded at this point and a crack formed near the fabric end. This end

crack widened with increasing load and propagated to the level of the internal steel reinforcement (Fig. 9b);

3) individual concrete cover blocks were formed between two adjacent cracks;
4) the end concrete cover block peeled away as the load increased (Fig. 9c);
5) This process continued sequentially for the rest of the blocks (Fig. 9d).

Due to the dowel action of the stirrups, the weakest plane forms right under the longitudinal steel reinforcement, thus, the peeling failure always started from the end of the plates and propagated along the concrete cover parallel to the longitudinal steel reinforcing bars.
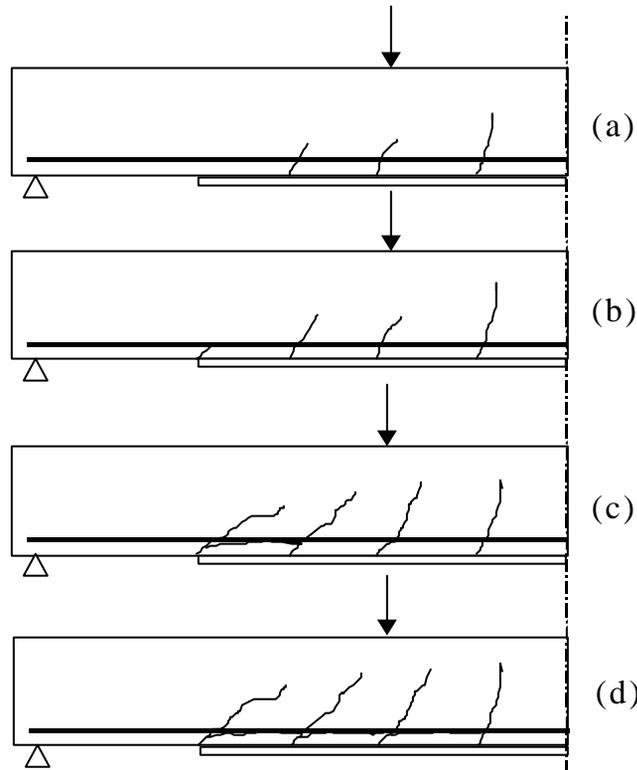

Fig. 9. Procedure of Peeling Failure Propagation

Debonding Failure

The beams with FRP fabric extending all the way to the support are subjected to lower stress concentrations at the FRP cutoff points and shear crack may not developed at these points. On the other hand, within the shear span, the shear stress concentration around the flexural or shear crack mouth displacements may also lead to the local debonding of the fabric along concrete-fabric interface (Fig. 10). Flexural cracks, located in regions of the beam with large moment, can initiate interfacial fracture which propagates between the concrete and FRP interface (Fig. 10b). Crack mouths located in regions of the beam with mixed shear and moments can subject an interfacial crack to mixed mode loading (Fig. 10c). For beam B3 with a long fabric covering almost the whole length of span, the debonding started at one of the flexural cracks in vicinity of the point load. The debonding propagated towards the sheet end until total delamination occurred.
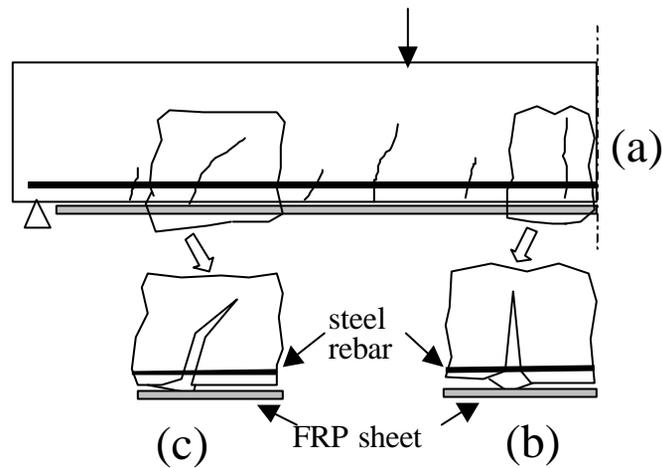
Fig. 10. Debonding failure between FRP fabric and concrete

In general, peeling of the concrete cover at the level of internal steel reinforcement occurred in beams with shorter fabric length where significant shear cracks were formed, indicating that significant stress concentration can occur at the sheet anchorage zone. Debonding failure between FRP fabric and concrete occurred due to susceptibility of the interface relative to vertical displacements of shear cracks in the concrete beam.

Strengthening Efficiency

The load-rebar strain responses are shown in Fig. 11. These curves terminated at the points where the electrical resistance strain gauges lost their effectiveness. The attached CFRP fabrics worked as external tensile reinforcement and share the applied load with internal steel reinforcement. It is shown that the rebars in the pure bending region enter the yield plateau for all the beams (the yielding strain for steel rebar was around 2500 microstrain). The load at which the steel yielded was higher for the strengthened beam, suggesting that internal forces were shared between the steel and FRP. Most of the increase in load-carrying capacity was obtained after the rebar yielding, indicating that FRP fabric works efficiently in tension after yielding of the rebar.
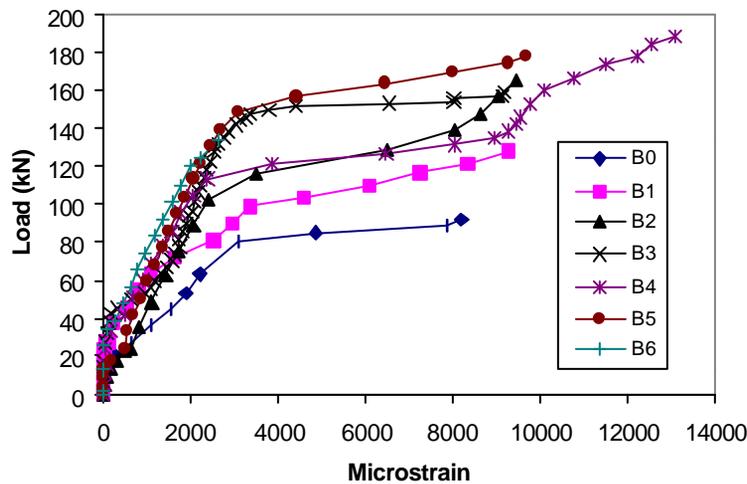

Fig. 11. Rebar Strain Response at the Mid-Span of Beams

The average ultimate strain in steel rebar (about 9000 microstrain) is more than 2.5 times the yield strain. This meets the current ductility requirement of ACI 440 F [14]. Therefore, it can be concluded that the beams undergo considerable deflections despite the eventual peeling of concrete cover and debonding of CFRP fabric that do occur abruptly. The average strain at failure in the FRP at the beam midspan was 45% of rupture strain (15,000 microstrain). For all strengthened specimens, the maximum strain recorded in the FRP fabric (beam B3 with a strain of 10,000 microstrain) was at best two-third of its ultimate value, indicating an inefficient use of material.

Conclusions

In general, the results of this experimental study showed that external bonding of CFRP fabrics to RC beams can increase the strength and stiffness with eventual peeling or debonding failure at ultimate. The following specific conclusions can be made for FRP strengthened beams.

1) The strength and stiffness of the beams were substantially increased. The ultimate load-carrying capacity of the beams increased by as much as 95% over their un-strengthened counterpart.
2) Pre-cracked and un-cracked beams exhibited similar characteristics.
3) The internal steel reinforcement ratio as well as the length and thickness of FRP fabrics are the major parameters that affect the performance of strengthened beams.
4) Peeling and debonding failures were prevalent in the tests conducted here. These failure modes were of brittle nature. The average ratio of the strain in the steel at the point of failure (including peeling and debonding) is about 2.5 times of the strain in steel at yielding. The beams were deformed considerably, even though the FRP fabrics were not fully utilized.
5) In comparison to conventional flexural failure modes, peeling and debonding failures are more difficult to characterize. Parameters other than shear and flexure influence the peeling and debonding failures. These parameters include epoxy thickness and their mechanical response, preparation of the concrete before application of the epoxy, and sensitivity to motions along member cracks propagating to the tension face.

Appendix: Ultimate flexural capacity of test beams

Control Beam

The ultimate moment of resistance of doubly reinforced concrete beam is

$$M_n = f_y(A_s - A_s') \left[d_s - \frac{f_y(A_s - A_s')}{2(0.85 f_c' b)} \right] + f_y A_s'(d_s - d') \tag{A.1}$$

Strengthened Beam

The minimum cross-sectional area of FRP to avoid FRP rupture failure is

$$c_f = d_f \frac{\varepsilon_{cu}}{\varepsilon_{cu} + \varepsilon_{fu}} \tag{A.2}$$

$$A_{f,min} = \frac{0.85 f_c' b \beta_1 c_f + A_s' f_s' - A_s f_y}{f_{fu}} \tag{A.3}$$

The maximum cross-sectional area of FRP to preclude concrete crushing failure is

$$c_b = d_s \frac{\varepsilon_{cu}}{\varepsilon_{cu} + \varepsilon_y} \tag{A.4}$$

$$A_{f,\max} = \frac{0.75(0.85 f_c' b \boldsymbol{b}_1 c_b) + A_s' f_s' - A_s f_y}{f_{fb}} \tag{A.5}$$

At ultimate state, the tension failure will be the yielding of the steel in tension followed by concrete crushing (Fig. A1). The ultimate moment of resistance after strengthening is
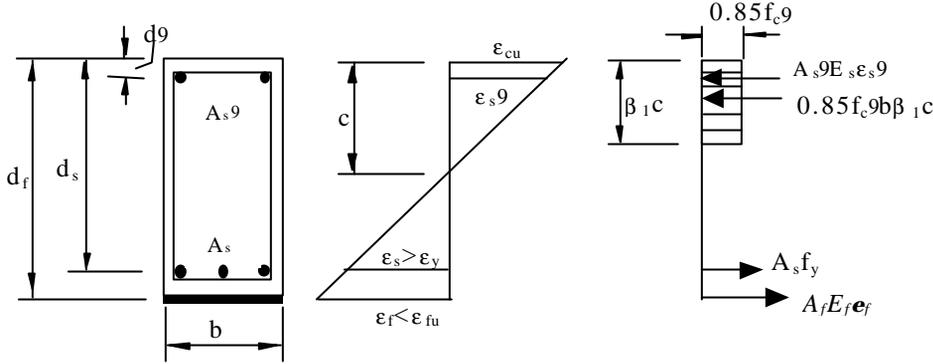

Fig. A1. Ultimate Condition Corresponding to Tension Failure

$$M_n = 0.85 f_c' b \boldsymbol{b}_1 c (d_f - \frac{\boldsymbol{b}_1 c}{2}) + A_s' E_s \boldsymbol{e}_s' (d_f - d') - A_s f_y (d_f - d_s) \tag{A.6}$$

c can solved by the following equation

$$c = \frac{-B_1 + \sqrt{B_1^2 - 4 A_1 C_1}}{2 A_1} \tag{A.7}$$

where $A_1 = 0.85 f_c' b \boldsymbol{b}_1$, $B_1 = -A_s f_y + (A_s' E_s + A_f E_f) \boldsymbol{e}_{cu}$, and $C_1 = -(A_s' E_s d' + A_f E_f d_f) \boldsymbol{e}_{cu}$.

References

1. Swamy, R. N. and Mukhopadhaya, P. (1999), "Debonding of Carbon Fiber Reinforced Polymer Plate from Concrete Beams", *Proc. Instn Civ Engrs Structs & Buldgs,* 134(4), pp. 301-317.
2. Sharif, A. M., Al-Sulaimani, G. J., Basunbul, I. A., Baluch, M. H., and Ghaleb, B. N. (1994), "Strengthening of Initially Loaded Reinforced Concrete Beams Using FRP Plates", *ACI Struct. J.,* 91(2), pp. 160-168.
3. Arduini, M., and Nanni, A. (1997), "Behavior of Precracked RC Beams Strengthened with Carbon FRP Sheets", *J. Compos. for Constr.,* ASCE, 1(2), pp. 63-70.
4. Arduini, M, Tommaso, A. D., and Nanni, A. (1997), "Brittle Failure in FRP Plate and Sheet Bonded Beams", *ACI Struct. J.,* 94(4), pp. 363-370.
5. Norris, T., Saadatmanesh, H., and Ehsani, M. R. (1997), "Shear and Flexural Strengthening of R/C Beams with Carbon Fiber Sheets", *J. Struct. Engrg.,* ASCE, 123(7), pp. 903-911.
6. GangaRao, H. V. S., and Vijay, P. V. (1998), "Bending Behavior of Concrete Beams Wrapped with Carbon Fabric", *J. Struct. Engrg,* ASCE, 124(1), pp. 3-10.
7. Ross, A., Jerome, D. M., Tedesco, J. W. and Hughes, M. L. (1999), "Strengthening of Reinforced Concrete Beams with Externally Bonded Composite Laminates", *ACI Struct. J.,* 96(2), pp. 212-220.
8. Rahimi, H., and Hutchinson, A. (2001), "Concrete Beams Strengthened with Externally Bonded FRP Plates", *J. Compos. for Constr.,* ASCE, 5(1), pp. 44-56.
9. Nguyen, D. M., Chan, T. K., and Cheong, H. K. (2001), "Brittle Failure and Bond Development Length of CFRP-Concrete Beams", *J. Compos. for Constr.,* ASCE, 5(1), pp. 12-17.

10. Spadea, G., Bencardina, F. and Swamy, R. N. (1998), "Structural Behavior of Composite RC Beams with Externally Bonded CFRP", *J. Compos. for Constr.*, ASCE, 2(3), pp. 132-136.
11. Ritchie, P. A., Thomas, D. A., Lu, LW. and Connelly, G. M. (1991), "External Reinforcement of Concrete Beams Using Fiber Reinforced Plastics", *ACI Struct. J.*, 88(4), pp. 490-500.
12. Bonacci, J. F., and Maalej, M. (2001), "Behavioral Trends of RC beams Strengthened with Externally Bonded FRP", *J. Compos. for Constr.*, ASCE, 5(2), pp. 102-113.
13. American Concrete Institute (ACI) (1999), "Building Code Requirements for Structural Concrete", ACI 318-99, Detroit.
14. ACI Committee 440 (2000), "Guide for the Design and Construction of Externally Bonded FRP System for Strengthening Concrete Structures", *ACI Committee 440-F Draft Document,* American Concrete Institute, Detroit.
15. El-Mihilmy M. T., and Tedesco, J. W. (2000), "Analysis of Reinforced Concrete Beams Strengthened with FRP Laminates", *J. Struct. Engrg*, ASCE, 126(6), pp. 684-691.
16. Park, R., and Paulay, T. (1975), "Reinforced Concrete Structures", *John wisley and Sons, Inc.,* New York, NY.

Notations

The following symbols are used in this paper:

A_f = Area of FRP reinforcement, mm^2

$A_{f,min}$ = minimum area of FRP reinforcement to preclude FRP rupture failure, mm^2

$A_{f,max}$ = maximum area of FRP reinforcement to avoid concrete crushing failure, mm^2

A_s = total area of longitudinal tension steel reinforcement, mm^2

A_s' = total area of longitudinal compression steel reinforcement, mm^2

b = width of a rectangular cross-section, mm

c = distance from extreme compression fiber to the neutral axis, mm

c_f = distance from extreme compression fiber to the neutral axis at the balanced condition of FRP rupture, mm

c_b = distance from extreme compression fiber to the neutral axis at the balanced condition of concrete crushing failure, mm

d_s = distance from extreme compression fiber to centroid of tension steel reinforcement, mm

d' = distance from extreme compression fiber to centroid of compression steel reinforcement, mm

d_f = distance from extreme compression fiber to centroid of FRP reinforcement, mm

E_c = modulus of elasticity of concrete, MPa

E_f = modulus of elasticity of FRP, MPa

E_s = modulus of elasticity of steel, MPa

f'_c = Specified compressive strength of concrete, MPa

f_{fb} = Stress in the FRP reinforcement in tension at the balanced condition of concrete crushing failure, MPa

f_{fu} = Design ultimate tension stress of the FRP system, MPa

f_s = Stress of the tension steel reinforcement, MPa

f_s' =   Stress of the compression steel reinforcement, MPa

f_y =   Specified yield stress of steel reinforcement, MPa

L_p =   Length of the FRP system, mm

L_0 =   Distance from the FRP system cutoff point to the support, mm

M_n =   Nominal moment capacity, kN-mm

P =   the sum of the two equal concentrated loads applied to the beams at failure, kN

$\boldsymbol{\beta}_1$ =   Ratio of the depth of the equivalent rectangular stress block to the depth to the neutral axis

$\boldsymbol{\varepsilon}_{cu}$ =   Ultimate strain of concrete

$\boldsymbol{\varepsilon}_f$ =   Strain in FRP reinforcement

$\boldsymbol{\varepsilon}_{fu}$ =   Design rupture strain of FRP reinforcement

$\boldsymbol{\varepsilon}_s$ =   Strain in tension steel reinforcement

$\boldsymbol{\varepsilon}_s'$ =   Strain in compression steel reinforcement

$\boldsymbol{\varepsilon}_y$ =   Yielding strain of steel reinforcement